LASER-PLASMA INTERACTION STUDIES USING ABOVE CRITICAL DENSITY GAS JET PLASMAS AND A MULTI-TW CO_2 LASER*

C. Gong, S. Tochitsky, J. Pigeon, C. Joshi, Neptune Laboratory, Department of Electrical Engineering, University of California Los Angeles, CA, 90095, USA

Abstract

CO_2 laser-plasma interaction provides a unique parameter space for particle acceleration in a gas jet plasma taking place at a critical plasma density $n_{cr} \sim 10^{19}$ cm^{-3} and even at higher densities (3~10 n_{cr}) of 10μm radiation. Here we report the latest results of our study of electron acceleration in a wide range of plasma densities 1~10 n_{cr} using a multi-TW CO_2 laser system at the UCLA Neptune Laboratory. To gain insight into plasma density profile evolution during ~120 ps long CO_2 laser-plasma interaction, we used laser interferometry with two 1 ps, 532 nm probe pulses with variable delay of 5~120 ps. The knowledge of spatial distribution of accelerated electron beam transported through the overdense gas plasma is critically important for minimizing laser beam filamentation and for understanding influence of other laser-plasma instabilities. This should allow for optimization of CO_2 laser driven shock wave acceleration of low-divergence monoenergetic ion beams [1].

INTRODUCTION

The interaction of short high-intensity laser pulses with an overdense plasma can produce forward directed multi-MeV ions and electrons. Electrons heated/accelerated by the laser pulse can drag ions with them due to the space charge separation. Studying the spatial distribution of accelerated electrons can help to optimize the quality and yield of ion beams and is also important for understanding laser-plasma instabilities.

At the UCLA Neptune laboratory, a ~120 ps CO_2 laser train of 3ps pulses separated by 18ps with a peak intensity up to ~4×10^{16} W/cm^2 is used to study overdense laser plasma interaction in a helium gas jet. One of our goals is to optimize the ion acceleration by collisionless shock waves [1]. In order to gain an insight into the plasma density profile evolution during the CO_2 laser pulse train, a two-frame interferometry using 1ps, 532nm light has been developed. An adjustable temporal delay 5~120ps between pulses allows for optical probing of the laser/plasma interaction region. Through a careful analysis and comparison of the two-frame interferogram, the hole boring speed of the above critical density layer pushed by the radiation pressure along the laser propagation axis can be measured. Also, forward directed electron and ion beam is recorded on the LANEX phosphor screen to analyse its spatial distribution and divergence. A permanent magnetic dipole with ~600 Gauss magnetic field is placed before the LANEX phosphor screen to estimate the energy of particle beams.

*Work supported by DOE grant DE-FG02-92-ER40727, NSF grant PHY-0936266 at UCLA

EXPERIMENTAL SETUP

Target Chamber

The CO_2 Master Oscillator Power Amplifier system having a multi-terawatt peak power is used in the experiment. Due to a modulated gain spectrum of the CO_2 molecule, a ~3ps CO_2 laser seed pulse evolves into a ~120ps long pulse train after amplification. Each individual pulse within the pulse train preserves the original pulse width and is separated from the adjacent pulse by ~18ps.

The experimental arrangement in a target chamber is shown in Fig. 1.

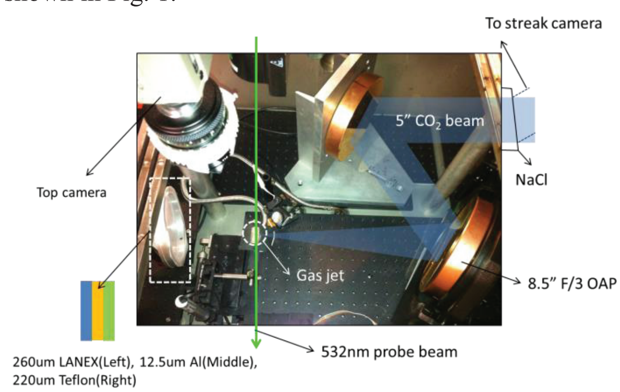

Figure 1: Experimental setup in the target chamber.

A 5” diameter CO_2 laser beam with an energy of ~60J is coupled into the target chamber through an 8” NaCl window mounted on a 4^o wedged flange. The back reflection of the beam from the salt window is combined with a red diode laser beam in a CS_2 Kerr modulator. The red pulse modulated by the high intensity 10μm CO_2 laser is analysed by a Hamamatsu streak camera (Model: C5680-21) for the temporal structure measurement of the CO_2 pulse. The beam inside the chamber is focused in a 2mm diameter gas jet by an 8.5” F/3 off-axis parabolic mirror. Using an IR camera, we have characterized the spatial profile of the unamplified CO_2 laser beam by scanning along the laser axis (Z-scan) which is shown in Fig. 2. The measured spot size is w_o = 48μm. Using this spot size and an estimate of the energy contained in the most intense of the 3ps pulses (~20%) in the train of pulses, we estimate that a peak a_o of >1 can be achieved in these experiment. Here a_o is the normalized vector

ISBN 978-3-95450-138-0

potential with a_o~1 corresponding to 10^{16} W/cm^2 for a CO_2 laser.

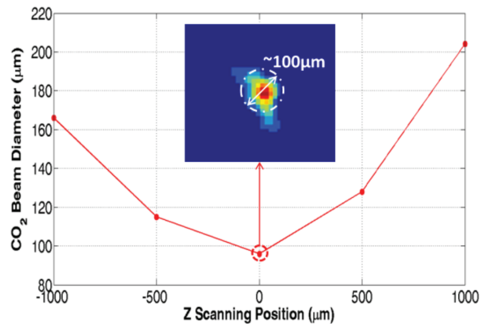

Figure 2: Spot size measurement of 10 µm CO_2 laser beam.

The laser beam interacts with a pulsed supersonic gas jet which allows for the peak plasma density around 0.1 to 10 times of the critical density for the 10µm light (10^{19} cm^{-3}).

As shown in Fig. 1, a detector consisting of a 260 µm LANEX phosphor screen (Left), 12.5 µm Al foil (Middle) and 220 µm Teflon (Right) layer is put 150mm away from the gas jet. The LANEX phosphor screen imaged by a COHU analog camera outside the target chamber is used to detect the forward directed electron beams with energy above 220keV. A permanent magnetic dipole (600 Gauss) capable of resolving energy in the range of 0.3-4 MeV is placed between the gas jet and the LANEX phosphor screen. A top COHU analog camera is installed to determine the focal position of the high power CO_2 beam relative to the center of the gas jet. A 1ps, 532nm, green probe with energy of ~20µJ is delivered to the interaction point (IP) for the two-frame interferometry and schlieren diagnostics.

Two-Frame Interferometry and Schlieren Diagnostics

The two-frame polarization based interferometry and schlieren optical scheme is depicted in Fig. 3.

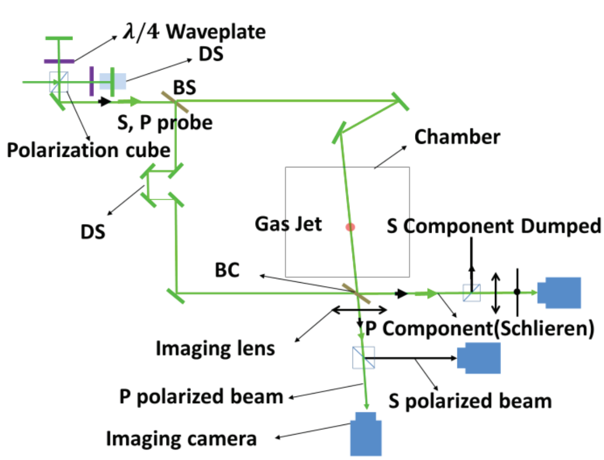

Figure 3: Schematic of the 1ps, 532nm two-frame interferometry and Schlieren diagnostics setup. Beam Splitter (BS), Delay Stage (DS), Beam Combiner (BC).

The 1ps, 532nm elliptically polarized probe beam enters the narrowband polarization cube and is separated into P (60%) and S (40%) components. This is a classical Michelson scheme in which an arbitrary delay can be introduced for the S polarized component. Then, each of them goes through a quarter wave plate twice and changes their polarization. A translational delay stage of the S probing arm is used to control the temporal delay relative to the P arm. The adjustable temporal range is 5~120ps with the P probe arriving at the IP earlier. After switching the polarization, P and S probes follow the same beam path and enter into the Mach-Zehnder interferometry system. Another narrow band polarization cube is placed behind BC to separate the polarized beams into two orthogonal directions. The imaging lens transfers the image plane of the plasma to the two CCD cameras. The measured spatial resolution of interferograms is ~20um. In addition to the interferometry, part of the beam probing the plasma is reflected off BC for a Schlieren diagnostic. The reflected beam contains P and S components and we use another polarization cube to select P component for the Schlieren image. A dark field schlieren technique [2] is used to analyse the plasma density gradient. A ~250um diameter ink dot deposited on a 2” transparent plastic disc is used as a beam stopper. The green probe passing through the plasma without refraction is attenuated by the dot by a factor of 10^5. The measured resolution of the schlieren images is ~40um.

EXPERIMENTAL RESULTS

At the Neptune laboratory, the 10um short pulse and the 532nm probe pulse are both produced using the same 1µm pulse [3], so inherently they are deterministically synchronized with each other. However, due to the different transport length, they arrive at the IP at different times and need to be temporally re-synchronized with a picosecond accuracy. Also as mentioned earlier, our structured CO_2 pulse train contains multiple ~3p micropulses separated by ~20ps. We are interested in observing the interaction between the overdense plasma and different micropulses in the pulse train and to learn how the plasma density profile will evolve temporally. To synchronize CO_2 laser pulse envelope and green probe with better than 20ps accuracy, a cross-correlation measurement in Si was used [4]. The probe timing of P arm is adjusted such that the probe pulse arrives approximately at the peak of the CO_2 pulse train. And the relative delay of the S arm can be changed using a delay stage in order to cover a chosen micro-pulse that arrives at a later time.

One of the most important mechanisms in laser overdense plasma interaction is hole boring or pushing of the density steepened plasma layer by radiation pressure of the laser field. Two frame interferometry allows for accurate measurement of the hole boring speed. For example, for interferogram shown in Fig. 4, we can extract this information by comparing how the overdense plasma layer is pushed by the radiation pressure at two different times.

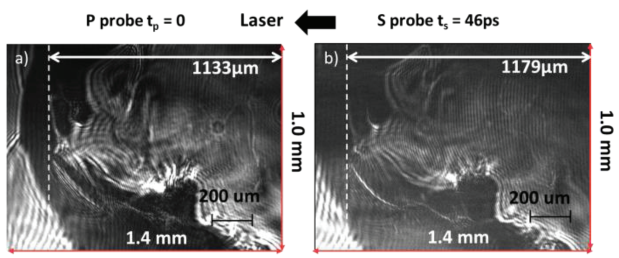

Figure 4: Two-frame interferogram at different times. a) shows P probe. b) shows S probe with 46ps delay. White dashed line shows the instantaneous position of the overdense plasma layer pushed by the radiation pressure.

For this shot our CO_2 laser beam is focused into a helium gas jet target and the laser intensity is above the ionization threshold of He^{2+} (~8.5×10^{15} W/cm^2). According to our neutral density calibration data of the gas jet, a backpressure of 1000psi corresponds to ~$6n_{cr}$ for a fully ionized He gas. Analysis of two interferograms of P and S arms (S is 46ps later) reveals that the pushed layer is moving forward with a hole boring velocity of 0.0037c (c is the speed of light).

Using the formula $\frac{v_h}{c} = [\frac{n_{cr}}{2n_{pe}}\frac{Zm}{M}\frac{I\lambda_L^2}{1.37\times10^{18}}]^{1/2}$ [5], where v_h is the hole boring velocity, n_{cr} the critical density for 10µm light, n_{pe} the plasma density and Z is the charge state of the ionized atoms, one can extract the laser intensity in the hole boring process which is 1.5×10^{16} W/cm^2. However, this formula assumes a constant radiation pressure and not directly applicable for the case of CO_2 laser 3ps pulses separated by 18ps. Thus, the intensity 1.5×10^{16} W/cm^2 corresponding to the measured v_h is a lower estimate of the laser intensity in the experiment.

Another shot, shown in Fig. 5, corresponds to the case when neutral density of the gas jet was reduced. We observed a nicely formed plasma channel. Analysis of the fringe shift in the interferogram gives us the plasma density in the channel of P probe time equal to 1×10^{18} cm^{-3} and S probe equal to 5×10^{17} cm^{-3}, which indicates a drop in plasma density over 46ps delay. Schlieren image in Fig. 5(c) shows a piled up plasma upstream of the plasma channel.

For this shot, a well-confined, beam-typed signal was detected on the LANEX screen with a divergence angle of 2^o. Currently, we are studying the nature and energy of this forward directed beam.

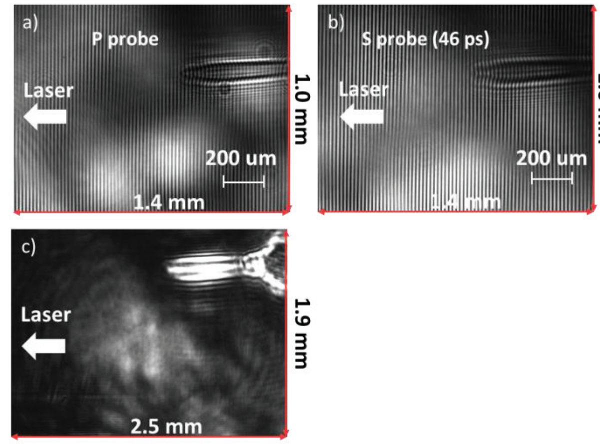

Figure 5: Two-frame interferogram and dark field schlieren images. a) Shows the channel formation as seen by P probing arm. b) Shows the channel expansion probed by S arm (46ps later). c) Shows the schlieren image for P polarized probe with a larger field of view.

CONCLUSION

In this paper, we describe the current status of the experiment being carried out in the Neptune laboratory at UCLA. Two-frame interferometry and dark field schlieren technique have been demonstrated to be very critical plasma interaction diagnostics. Hole boring velocity has been measured by comparing two interferogram images taken at different time. A channel guided propagation of laser light is observed at the underdense plasma condition and the corresponding signal on the LANEX phosphor screen requires further investigation.

REFERENCES

[1] Haberberger, et al. 2012 Collisionless shocks in a laser-produced plasma generate monoenergetic high-energy proton beams. Nat.Phys. 8, 95–99.

[2] G.S. Settles, *Schlieren and Shadowgraph Techniques* (Springer-Verlag, Berlin, 2001).

[3] D. Haberberger et al., Opt. Exp. 18, 17865 (2010).

[4] A.J. Alcock and P.B. Corkum, “Ultra-fast switching of infrared radiation by laser produced carriers in semiconductors,” *Can. J. Phys*., vol. 57, p. 1280, 1979.

[5] S.C. Wilks, et al. “Absorption of Ultra-intense Laser Pulse”, PRL, Vol. 69, Number 9.

ISBN 978-3-95450-138-0